Tol Energy-Driven Localization of Pal and Anchoring to the Peptidoglycan Promote Outer-Membrane Constriction

Melissa Petiti, Bastien Serrano, Laura Faure, Roland Lloubes, Tam Mignot, Denis Duché

Tol energy-driven localization of Pal and anchoring to the peptidoglycan promote outer membrane constriction

Mélissa PETITI[1], Bastien SERRANO[1], Laura FAURE[2], Roland LLOUBES[1], Tâm MIGNOT[2] and Denis DUCHE[1#]

1 - Laboratoire d'Ingénierie des Systèmes Macromoléculaires, UMR7255, Institut de Microbiologie de la Méditerranée, Aix-Marseille Univ - CNRS, Marseille, France.

2 - Laboratoire de Chimie Bactérienne, UMR7283, Institut de Microbiologie de la Méditerranée, Aix-Marseille Univ - CNRS, Marseille, France.

Running title: **Energy state of Tol-Pal and cell division**

Correspondence address: CNRS - LISM - UMR7255, 31 chemin Joseph Aiguier 13402 Marseille Cedex 20, France; Phone: +33 (0)4 91 16 41 56; Fax: +33 (0)4 91 71 21 24; duche@imm.cnrs.fr

Abstract

During cell division, Gram-negative bacteria must coordinate inner membrane (IM) invagination, peptidoglycan (PG) synthesis and cleavage and outer membrane (OM) constriction. The OM constriction remains largely enigmatic and the nature of this process, passive or active, is under debate. The proton-motive force (PMF) dependent Tol-Pal system performs a network of interactions within these three compartments. Here we confirm that the trans-envelope Tol-Pal complex accumulates at constriction site in *Escherichia coli.* We show that the IM complex composed of TolA, TolQ and TolR recruits the OM complex TolB-Pal to the septum, in an energy-dependent process. Pal recruitment then allows its binding to PG and subsequently, OM constriction. Our results provide evidence that the constriction of the OM is an energized process.

Keywords: molecular motor, Tol-Pal system, septum, OM invagination, membrane vesicles

Abbreviations used: OM, outer membrane; IM, inner membrane; PG, peptidoglycan; PMF, proton-motive force; sfGFP, super-folder green fluorescent protein; OmpA, outer-membrane protein A; Lpp, Braun's lipoprotein

Introduction

Gram-negative bacteria evolved a complex bacterial envelope consisting of two membranes, the inner (IM) and outer (OM) membranes, confining a periplasmic space in which a thin layer of PG resides. This three-layer structure acts as a physical and selective barrier against noxious compounds and contributes to mechanical robustness of the cell [1]. Cell division is the last event of the bacterial cell cycle and requires a coordinated constriction of these three layers to maintain the cell envelope integrity.

In *E. coli*, cell division is a highly coordinated dynamic process involving more than 30 different proteins that form a large complex called the divisome. Assembly of the divisome at midcell is initiated by association of three proteins: a cytoplasmic protein FtsZ, a bitopic IM protein ZipA and an associated IM protein FtsA, which form a dynamic ring structure commonly referred as the proto-ring or the Z-ring. After a temporary delay, seven additional essential proteins, FtsK, FtsQ, FtsL, FtsB, FtsW, FtsI and FtsN are recruited to the proto-ring to complete the division machinery which ultimately extends from the cytoplasm to the three layers of the cellular envelope. Once the full divisome is assembled, the synthesis of septal PG starts driven by treadmilling of FtsZ filament bundles, which is coordinated with IM constriction and the constitution of the septum (for reviews see [2-5]). How Gram-negative bacteria coordinate OM invagination with IM invagination and septal synthesis remains largely unknown.

The Tol-Pal system is a trans-envelope complex highly conserved among gram-negative bacteria. The core of this system is composed of five proteins organized in two sub-complexes. The IM complex is composed of three proteins: the proton channel-forming TolQ, TolR and associated TolA anchored in the IM, while the OM complex is composed of TolB, a periplasmic protein, and Pal a lipoprotein anchored in the inner leaflet of the OM and able to bind the PG layer (Fig. 1a). *In vivo,* the two sub-complexes are transiently connected by TolA. TolA has a long predicted helical second domain (TolAII) that is thought to stretch across the periplasm where its C-terminal domain interacts with TolB N-terminal domain and potentially also with Pal in a PMF-dependent manner [6]. Thus, the Tol-Pal complex uses the PMF to form a link between the IM and OM. In *E. coli,* two additional proteins are encoded in the *tol-pal*

cluster (Fig. 1b): the cytoplasmic thioesterase YbgC and the periplasmic protein CpoB [7].

Previous results suggest that the Tol-Pal complex could play a key role in the OM constriction. This complex transiently links the three layers of the cell envelope [6, 8-12], accumulates at the septum during cell division [13] and CpoB encoded by the last gene of the *tol-Pal* cluster, has been described to regulate activity of a major PG synthase (PBP1B) in response to the Tol energy state [7]. These results suggest that OM constriction could be an active process dependent of the Tol-Pal system. Despite this potential essential role, the cellular localization of the Tol-Pal complex in *E. coli* has been analyzed under multicopy production of Tol-Pal fluorescent derivatives [13] while the role of the energy state of the Tol-Pal complex in its localization has not been documented.

The PMF, TolQ and TolR proteins and the trans-membrane helix of TolA regulate the conformational change of the periplasmic region of TolA, and probably its ability to interact with Pal and perhaps TolB [6]. The TolQ-R complex is part of an emerging molecular motor family which is able to convert chemical energy derived from the PMF to mechanical movements [14]. This molecular motor family includes several multiprotein complexes that share sequence and conformational similarities. The MotA/MotB proteins drive the bacterial flagellum, the ExbB/ExbD proteins are involved in iron uptake and the recently characterized AglSQR proteins drive *M. xanthus* gliding motility; all work as motors as they convert chemical energy (PMF) into mechanical movement in order to energize a TolA-like partner [15-17]. Paradoxically and in contrast to other Tol-like motors, the exact function of the Tol-Pal system remains enigmatic, essentially because of the pleiotropic phenotypes exhibited by the *tol* mutants [18-24], and in particular the exact contribution of Tol-Pal to cell division remains obscure [21,25].

In this study, we revisited the question of the Tol-Pal proteins localization. In order to monitor the intracellular localization and dynamic of each Tol-Pal protein during the cell cycle, we initiated a systematic fluorescence microscopy approach in *E. coli*. To further gain insight on how this machinery operates, we engineered chimeric proteins expressed from their endogenous chromosomal loci, fused to fluorescent markers such as sfGFP or mCherry. Only the core proteins of the Tol-Pal system that are conserved among Gram-negative bacteria were studied. In the first part of this paper

we showed that all the chimeric proteins were functional and stably produced. We confirmed that the Tol-Pal proteins are dynamically recruited to the constriction sites during cell division. In addition, we showed that TolR requires either TolA or TolQ for its localization whereas TolA and TolQ localize independently of any of the other Tol-Pal proteins. Strikingly, TolQ, TolR, TolA, and TolB are absolutely required for Pal association with division sites, an active recruitment process that requires the PMF. Finally, the PG binding domain of Pal is not required for its septal localization, but absolutely require for its function and for proper OM constriction during cell division.

Results

Chromosomal-encoded fusion of the Tol-Pal components to fluorescent domains results in functional fluorescent proteins.

To further gain information on the cellular localization of Tol-Pal components, their recruitment and dynamic behavior, we engineered strains producing super-folder GFP (sfGFP) or mCherry fused to the N or C terminus of TolQ, TolR, TolA, TolB, and Pal. All the constructs were introduced at their respective native locus on the chromosome. sfGFP was fused to the cytoplasmic N-terminus of TolA and TolR. Indeed, the C-terminal domain of TolA and TolR has been described to be involved in many interactions with the others proteins of the complex and the proximity of a fluorescent marker might inhibit their function (for a review see [26]). As mCherry-protein fusions have been described to be effectively transported to the periplasm of *E. coli* for protein localization experiments [27], this fluorescent marker was fused to the C-terminus of TolB, Pal and also to the cytoplasmic C-terminus of TolQ. The distal N-terminal part of TolB contains the TolA binding site and is therefore not suitable to fuse a fluorescent marker [28].

We first checked that all the fluorescent Tol-Pal fusions proteins were functional. It has been previously described that Tol-Pal mutants are hypersensitive to detergents [29], form cell chains in medium of low osmolarity [25] and are resistant to colicins [30]. Here we showed that all the strains producing a fluorescent Tol-Pal fusion protein displayed a wild-type phenotype (Table 1 and Fig. 2 and S1-3). These strains were able to grow as efficiently as the wild-type strain in presence of SDS (Fig. 2a and S1), did not form cell chains in LB medium lacking NaCl (Fig. 2b and S2), and were sensitive to different colicin concentrations (Fig. 2c and S3), in contrast to the strain W3110 deleted of the *tolA* gene (Table 1 and Figs. 2a-c, and S1-3). These results clearly showed that all the fluorescent Tol-Pal fusion proteins remained functional.

The *tol-pal* genes are transcribed as two distinct operons, *ybgC tolQRA* and *tolB pal cpoB* [31] (Fig. 1b). As shown in figure 2d by immunoblotting analysis with the indicated antibodies, insertion of sfGFP or mCherry coding sequence in these operons did not modify the level of expression of the resulting chimeric fluorescent proteins, as well as the level of expression of the others proteins of the Tol-Pal

complex. Nevertheless, the strain producing TolB-mCherry was associated with a decrease in Pal abundance. This decrease does not interfere with Tol-Pal function because the strain producing TolB-mCherry displayed a wild-type phenotype, absence of filamentation, growth on detergent and sensitivity to colicin A similar to the W3110 strain (Table 1 and Figs. S1-3). We therefore used that strain throughout this study.

Tol-Pal proteins are recruited to cell constriction site.

The intracellular localization of each of the Tol-Pal proteins fused to a fluorescent reporter was analyzed by a live fluorescence microscopy approach. Time-lapse microscopy recordings showed that all tested fluorescent Tol-Pal proteins first appeared diffuse in the cell and were dynamically recruited to future division sites during cell division until they dispersed after daughter cell separation (Fig. 3a, left panel). Notably, Pal-mCherry remained longer than the other Tol proteins at the new cell poles (Fig. 3a, right panel). These results were confirmed by Kymograph analysis (Fig. 3a, right panel) and a large-scale demograph analysis of cells (Fig. 3b). While the demograph analysis (Fig. 3b) may suggest that there is a temporal pattern in the mid-cell recruitment of the Tol proteins during cell cycle, we believe that our data cannot be used to confirm or infirm this hypothesis. Indeed, the number of Pal molecules per cell has been estimated between 30,000 to 40,000 copies, whereas the number of TolA molecules per cell has been estimated between 400 to 800 copies [26]. These differences of abundance make it easier, for example, to detect Pal at the septum. The precise timing interpretation of the Tol-Pal protein localisation would require a more stringent analysis of cell fluorescence, specifically the analysis of dual-labelled strains. Nevertheless, based on the recordings presented on Fig 3, our results confirm unambiguously that the Tol-Pal proteins are recruited to the septum during cell division.

TolR requires TolA or TolQ for its localization at the cell constriction site.

To determine the role of each Tol-Pal proteins in the assembly of the core-complex and their recruitment to the septum, we analyzed the intracellular localization of the different chimeric fluorescent proteins in various deletion mutant

backgrounds. Each of these deletion mutants, *tolA, tolB, tolQ, tolR, tolQR and pal,* present a classical *tol* phenotype (Table 1 and Figs. S1-3). Western blot analysis confirmed deletion of each *tol-pal* gene and showed that *tolB* and *tolQ* deletions led to a reduced production of Pal and of TolR, respectively. The level of production of the others proteins were not affected (Fig. S4) First, we analyzed the behavior of the three IM proteins of the Tol-Pal complex, TolA, TolQ and TolR, during cell division. Using plasmid encoded fluorescent fusions, Gerding and co-workers previously reported that GFP-TolA and TolQ-GFP, but not GFP-TolR localize at the septum in a TolQ-R-A-B-Pal mutant background [13]. Here, we deciphered further the Tol recruitment process, showing that sfGFP-TolA, TolQ-mCherry and sfGFP-TolR accumulated at the constriction sites in all single deletion mutants tested. These data demonstrate that assembly of a functional molecular motor is not required for recruitment of the Tol-Pal proteins to the septum (Figs 4a-c). It has been previously described by crosslinking experiments that TolR can interact with TolQ in absence of TolA and with TolA in absence of TolQ [9,32]. Thus, although TolA and TolQ do not require any Tol-Pal protein for their septal location, and based on previous observations [13], it is likely that TolR requires either TolA or TolQ for its recruitment to the septum (Fig. 4b).

Pal requires the TolQ, TolR, TolA and TolB proteins and a functional TolQ-TolR molecular motor for its localization at the cell constriction site.

The Tol-Pal OM complex is composed of the OM anchored lipoprotein Pal and the soluble periplasmic TolB protein. TolB-mCherry also localized to the division septum (Fig. 5a). In the various *tol-pal* deletion mutants, TolB-mCherry was largely sequestered in apparent membrane vesicles that formed at constriction sites (Fig. 5b). This could be expected because *tol-pal* mutants have been previously reported to show pleiotropic phenotypes, including pronounced local expansions of their periplasmic space at sites of constriction and abundant vesicle formations [13,33,34]. To test whether periplasmic proteins could indeed be detected in vesicles, we also imaged a GFP protein fused to a Tat signal peptide (Tat-GFP), a periplasmic control protein, in WT and *tol-pal* mutant cells (Fig. 5a, 5b). In a wild-type background, Tat-GFP was localized all around the cell envelope suggesting that it is indeed homogeneously distributed in the periplasmic space. However, we observed

numerous highly fluorescent vesicles emerging from the constriction sites or located at the pole of the *tol-pal* mutant cells (Fig. 5b).

The intracellular localization of Pal in the different mutant backgrounds revealed that Pal-mCherry was not recruited at the constriction sites during cell division but remained spread in the OM (Fig. 5c). This result demonstrates that recruitment of Pal-mCherry to division sites requires all the Tol proteins. TolA interacts with Pal in a PMF-dependent manner (directly or via TolB, see below), and this interaction is regulated by the molecular motor TolQR. It has been previously described that a single D23A mutation in the transmembrane segment of TolR deactivates the TolQR motor without affecting TolQR-TolA complex assembly [35]. When we complemented, a *tolQR* strain with a plasmid encoding TolQR, Pal-mCherry was recruited to the septum (Fig. 5c). However, introduction of a plasmid encoding $TolQR_{D23A}$ failed to restore septal localization and Pal-mCherry was dispersed along the periphery of the cell (Fig. 5c). These results show that a functional TolQR motor is absolutely required to maintain Pal at the septum.

Key role of Pal at the septum.

Previous studies demonstrated that Pal interacts both with TolB and the PG, and that these two interactions are mutually exclusive [10,11]. To analyze the role of Pal at the septum we first constructed a plasmid encoding the fluorescent hybrid protein Pal-sfGFP under the control of an arabinose inducible promotor and verified that this construction was correctly expressed, functional (Fig. 6a-c and Table 1) and localized at the constriction sites during cell division (Fig. 6e, WT panel). Then, we constructed two mutated version of Pal-sfGFP (Fig. 6d). A Pal (E102K) variant that prevents Pal-TolB interaction but does not affect PG-binding and a Pal (R104C) variant that interacts with TolB but does not bind PG [36]. The two mutated Pal-sfGFP proteins (Pal_{102}-sfGFP and Pal_{104}-sfGFP) were correctly expressed (Fig. 6a) but as previously shown were not able to complement a Δ*pal* strain [36] (Fig. 6b, c and Table 1). Thus, Δ*pal* strain producing either Pal_{102}-sfGFP or Pal_{104}-sfGFP fusion protein showed a high sensitivity to detergents (Fig. 6c) and showed a chaining phenotype under low osmolarity growth conditions indicative of a division and cell separation defect (Fig. 6b). The Pal_{102}-sfGFP did not localize at the sites of constriction during cell division, indicating that interaction with TolB is essential for Pal recruitment (Fig. 6e). In

contrast, Pal_{104}-sfGFP localized at the septum normally, indicating that once at the septum, Pal must interact with the PG to perform its function. Finally, in a *ΔtolB-pal* strain, Pal_{104}-sfGFP showed no septal localization during cell division (Fig. 6e). These results clearly indicate that TolB is absolutely necessary for functional Pal localization and that Pal binding to PG is absolutely necessary to the function of the Tol-Pal system in cell division.

Discussion.

Cell division in Gram-negative bacteria is orchestrated by the divisome and requires the coordinated constriction of the three cell envelope layers. Despite major progress understanding IM invagination, little is known about OM coordinated constriction. It has been suspected for a long time that OM invagination during cell division might be achieved passively, by simple tethering of OM lipoproteins to the PG. However recent evidence suggested a potential role of the Tol-Pal complex in cell division and particularly in OM constriction. The Tol-Pal proteins connect the three layers of the cell envelope [26], and they have been described to localize at the septum during cell division [13]. Interestingly, although Pal is a PG-binding OM lipoprotein, it is not covalently attached to the PG. Pal is engaged in many interactions with different partners, localized in the OM, the periplasm and the IM, and some of these interactions are exclusive. Moreover, interaction between TolA and Pal requires the PMF and a functional TolQR molecular motor [14]. These data led the hypothesis that Pal might facilitate an active mechanism of OM constriction during cell division

Here, we revisited the localization of the Tol-Pal system during cell division and provided information on the impact of the TolQR motor and the Pal PG binding site in Pal localization and function. To overcome possible artefacts resulting from overexpression of chimeric fluorescent proteins encoded by plasmids, we engineered strains producing super-folder GFP (sf-GFP) or mCherry fused to the N- or C-terminus of the Tol-Pal proteins (Table S1). All these chromosomal constructs were introduced at the native, original loci. We first checked that all constructions were functional and expressed at their original level (Fig. 2 and Table 1). Time lapse experiments clearly indicate a dynamic septal recruitment of the Tol-Pal proteins during cell division (Fig. 3a). In non-constrictive cells, each of the Tol-Pal protein appears dispersed in the cell envelope, then begins to accumulate at the septum during cells constriction and finally disperses again after cell separation. Demograph analysis of cells producing the different fluorescent chimeric Tol-Pal proteins confirm this result (Fig. 3b).

Interestingly we observe that TolQ and TolA accumulate at the constrictions site independently of the other Tol-Pal proteins and that Pal absolutely requires all the Tol proteins to be associated with the cell septum (Fig. 4, 5). Based on these results and

previously published results, it seems likely that the IM TolQRA complex is first recruited by either FtsN for TolQ [37] or an active divisome complex for TolA [7,13,38]. TolR is able to directly interact with TolA or TolQ and therefore its septal localization is likely dependent of one of these two proteins. Once in mid-cell, the TolQRA complex and TolB drive the recruitment of Pal at the division site. However, from our results, it is not possible to conclude decisively whether the TolQRA complex recruits a TolB-Pal OM complex or whether it first recruits TolB, which then recruits Pal. TolA could also interact directly with Pal, although this interaction cannot overcome the requirement for TolB. In fact, previous papers indicate contradictory results about the TolA-Pal interaction. Based on a co-immunoprecipitation approach, TolA and Pal have been described to interact *in vivo* through a PMF-dependent mechanism [6,39]. However, such interaction was not detected *in vitro* with purified proteins by isothermal calorimetry (ITC) [28] suggesting that the TolA-Pal interaction could be indirect (*i.e.*, mediated via TolB). In a previous paper [13], the authors speculated that TolB could reverse Pal-PG interactions to permit lateral movement of the lipoprotein in the OM and then its interaction with TolA at the division site. However, this is unlikely because we show here that the mutated Pal_{R104C} that does not bind the PG and is free to diffuse in the OM is not localized at the division site in the absence of TolB (Fig. 6e). Thus, TolB is required for Pal to localize to the septum likely via direct recruitment.

In addition, we demonstrate that the energy provided by a functional TolQR complex is absolutely require for a correct localization of Pal during the cell cycle. Indeed, in the absence of TolQR or in the presence of a defective $TolQR_{D23A}$ complex, unable to energize TolA, Pal localized all around the cell envelope and does not accumulate at the constriction site during cell division (Fig. 5c). Thus, the septal recruitment of Pal is a PMF-dependent process. Based on these results, we propose a model for Tol-Pal function during cell division. First, the IM TolQRA complex is recruited to the division site by divisome proteins (*i.e.,* FtsN and others). Second, the motor becomes active and energizes TolA to recruit the OM TolB-Pal complex. Such transient ternary complex has been previously observed although in low yield by *in vitro* cross-linking experiment with purified proteins [28]. It is possible that the mechanical action of the TolQR motor, allows TolA to pull the TolB-Pal complex inwards, drawing the outer membrane invagination over to the PG and IM layers. Completing this cycle, TolA would dissociate TolB from Pal, thus permitting

Pal-PG interaction. Indeed, the large differences of affinity between the TolB-Pal (nM) and TolA-TolB (µM) interactions [28] are not in favor of a TolA-TolB association. In conclusion, this cycle of exclusive TolA, TolB and Pal interactions and the contractile activity of Tol-Pal complex regulated by the energy state of the TolQR motor, would maintain sufficient contact between the three layers of the envelope for efficient invagination. In addition, the energy state of the Tol-Pal complex has already been involved in the regulation of the PBP1B-LpoB machine involved in PG synthesis at constriction sites [7]. Thus, the Tol-Pal complex appears to regulate and coordinate septal PG synthesis and OM constriction. Surprisingly, *in E. coli*, despite all the phenotypes associated with the *tol* mutations and the role of the Tol-Pal complex in the cell division, this complex is not essential for viability in standard laboratory conditions, suggesting that the Tol-Pal function, at least in the cell division, could be compensated by another trans-envelope complex. Indeed two global approaches, have shown that mutations in Tol-Pal complex are synthetically lethal when combined with mutations in the trans-envelope complex, LpoB-PBP1B [40]. This complex also seems to participate in tethering the OM either to the PG or the IM and localizes at constriction sites, likely promoting OM constriction during cell division even when Tol-Pal is absent, in standard laboratory conditions [40]. In low osmolarity media, where Tol-Pal is essential, the energy provided by the TolQR motor and the elongated TolAII domain could prevent local expansions of the periplasmic space which is harmful to complete the cell division.

Although the Tol-Pal localization at the septum during the cell cycle is clearly established, many questions remain unanswered. Which proteins recruit the Tol-Pal complex at the septum? FtsN is a good candidate for TolQ and has been previously described to be involved in the recruitment of TolA [13,37]. However, the role of FtsN in the recruitment of TolA could be indirect, because a suppressor mutation in FtsA can restore the correct localization of TolA and function of the Tol-Pal system in a FtsN-depleted strain [38]. Similarly, the direct recruitment of TolQ by FtsN is questionable. Another major interrogation concerns the timing and sequence of the interactions between TolA, TolB, Pal and the PG driven and cycled as function of the energy state of the system. Understanding and deciphering these interaction networks would greatly improve our knowledge on the Tol-Pal system function at the septum during the cell division.

Acknowledgements— We thank Annick Brun, Isabelle Bringer, Moly Ba, Olivier Uderso for technical assistance, Sacha Touille for encouragements and Laetitia Houot for carefully reading the manuscript. Work in RL. laboratory is supported by the Centre National de la Recherche Scientifique (CNRS) and the Aix-Marseille Univ. R.L. research team is supported by Agence Nationale de la Recherche (MEMOX, ANR-18-CE11).

Conflict of interest—The authors declare that they have no conflicts of interest with the contents of this article.

Material and Methods

Bacterial strains, plasmids, and growth

Strains, and plasmids used for this study are listed in Table S1. *E. coli* strains were grown aerobically at 37°C in Lysogeny Broth medium or at 30°C in M9 minimum medium, supplemented with antibiotics if necessary (ampicillin 100 µg/ml, kanamycin 50 µg/ml and/or chloramphenicol 30 µg/ml).

Plasmid construction

PCRs were performed in a Biometra thermocycler, using Pfu Turbo DNA polymerase (Stratagene, La Jolla, CA). Oligonucleotides were synthesized by Sigma. Plasmids pTolQR and pPal were constructed by a double PCR technique [41], allowing amplification of the *tolQR* and *pal* genes, flanked by extensions annealing to the target vector (pBad/HisC). The product of the first PCR was then used as oligonucleotides for a second PCR with the target vector as a template. Plasmid pPal-sfGFP was constructed by a double PCR technique, allowing amplification of the *sfGFP* gene, flanked by extensions annealing to the target vector (pPal). Site-directed substitutions were introduced by QuikChange mutagenesis PCR using complementary pairs of oligonucleotides.

Cloning and expression of *E. coli* Tol-Pal proteins

The *E. coli* W3110 strains carrying the chromosomal gene deletions or tags of interest were obtained using a modified protocol from Datsenko & Wanner [42] as described previously [43]. Briefly, for each gene deletion, a kanamycin cassette was amplified from the vector pKD4 using a pair of oligonucleotides carrying 50-nucleotide extensions homologous to regions that are adjacent to the target gene. After electroporation of the PCR product into *E.coli* W3110 cells carrying the pKOBEG vector, kanamycin-resistant clones were selected and confirmed by colony-PCR. The kanamycin cassette was then excised using vector pCP20 and gene deletions were verified by PCR. The same procedure was performed to introduce the mCherry or sfGFP coding sequences upstream the stop codon (pKD4-*sfgfp* or pkD4-

mCherry) or downstream from the start codon (p*gfp*-KD4 or p*mCherry*-KD4), resulting in strains producing fusion proteins from their native chromosomal loci.

Western Blots and protein production

Protein production from gene expression at chromosomal loci was checked by western blot experiments on over-night cultures. Heat treated samples (A_{600} = 0.2) were loaded on 12,5% SDS-PAGE and analyzed by western-blot immunodetection using specific antibodies. When necessary, plasmid multicopy expression was induced with arabinose 0,02% for 1 hour.

Fluorescence microscopy

Overnight cultures of *E. coli* W3110 wild-type or derivative strains were diluted to A_{600} ~ 0.1 in M9 minimum medium supplemented with glucose and casa-amino acids and grown at 30°C with agitation to reach an A_{600} ~ 0.6. Cells were washed twice and resuspended in the same medium to an A_{600} ~ 0,6 and spotted on a cover slip and covered with a thin pad of 1.5% agar in M9 minimum medium supplemented with glucose and casa-amino acids.

Time-lapse fluorescent experiments

For each time-lapse experiment, four independent fields were manually defined with a motorized stage (Prior Scientific) and stored (X, Y, Z, PFS-offset) in a custom automation system designed for time-lapse experiments. Fluorescence and phase contrast images were captured every 2 minutes using an automated and inverted epifluorescence microscope TE2000-E-PFS (Nikon, France) equipped with Perfect Focus System (PFS) during 2 hours. PFS automatically maintains focus in order to keep in sharp focus the point of interest at all times and despite mechanical or thermal perturbations. Images were recorded with a CoolSNAP HQ 2 (Roper Scientific, Roper Scientific SARL, France) and a 100X/1.4 DLL objective. Excitation light was emitted by a 120-watt metal halide light. The sfGFP images were recorded by using the ET-GFP filter set (Chroma 49002) using an exposure time of 500–700 ms and the mCherry images were recorded by using the ET-mCherry filter set

(Chroma 49008) using an exposure time of 100–700 ms. Phase contrast and fluorescence channels were adjusted and merged using the Fiji software (http://rsb.info.nih.gov/ij/). Some slight movements of the whole field during the experiments were corrected by registering individual frames using 'StackReg' and 'Image Stabilizer' plugins for ImageJ.

One-shot acquisitions

Fluorescence and phase contrast images were captured and recorded with the same devices described previously, using an exposure time of 1500 ms for mCherry and sfGFP images.

Statistical analysis

First, noise and background were reduced using the 'Subtract Background' plugin from Fiji. Cells and fluorescent foci were automatically detected with MicrobeJ plugin for ImageJ (http://www.microbej.com). To avoid false positive, each event was manually controlled in the original raw data. Kymograph representations were made using the 'KymoResliceWide' plugin from Fiji and demograph or Heatmap representations were made with the 'Demograph' or 'Heatmap' options from MicrobeJ.

Phenotypic studies

Phenotypic studies have been performed in order to visualize effects of the fluorescent markers chromosomal insertion and gene deletions onto the *tol-pal* operon. Three assays were achieved to check the OM integrity, the Tol-Pal complex assembly and the cell division process. *Colicin tolerance assay:* Colicin A and D lethal activities were checked by the presence of halos on a cell lawn of the strain to be tested, as previously described [44]. Data are reported in Table 1 as the maximal dilution of the colicin stock sufficient for inhibiting cell growth and are showed in Fig. S3). *SDS sensitivity assay:* Sensitivity to Sodium Dodecyl Sulfate (SDS) was determined by measuring the level of survival of the strain after 4 hours of incubation at 37°C in liquid LB medium containing various concentration of SDS (from 0.5% to

2%). Data are reported in Table 1 as “S” for sensitive strains or “R” for resistant strains and also in Fig S1 and S5. *Cell division assay:* Cells were grown for 4 hours at 37°C in LB (171 mM NaCl) or LB–NaCl (0 mM NaCl) liquid medium. Then cells were fixed on fresh Poly-L-Lysine (0,1% w/v in H_2O) coated microscope slides and were observed with an optical microscope (Eclipse 50i, Nikon, France).

References

1. H. Nikaido, Molecular basis of bacterial outer membrane permeability revisited, Microbiol. Mol. Biol. Rev. 67 (2003) 593-656.
2. P.A. de Boer, Advances in understanding E. coli cell fission, Curr. Opin. Microbiol. 13 (2010) 730-737.
3. A.J. Egan, W. Vollmer, The physiology of bacterial cell division. Ann N Y Acad Sci. 1277 (2013) 8-28.
4. M.J. Tsang, T.G. Bernhardt, Guiding divisome assembly and controlling its activity. Curr. Opin. Microbiol. 24 (2015) 60-65.
5. D.P. Haeusser, W. Margolin, Structural and functional insights into the dynamic bacterial Z ring, Nat. Rev. Microbiol. 14 (2016) 305-319.
6. E. Cascales, M. Gavioli, J.N. Sturgis, R. Lloubes, Proton-motive force drives the interaction of the inner membrane TolA and outer membrane Pal proteins in *Escherichia coli*, Mol. Microbiol. 38 (2000) 904-915.
7. A.N. Gray, A.J. Egan, I.L. Van't Veer, J. Verheul, A. Colavin, A. Koumoutsi, J. Biboy, A.F. Altelaar, M.J. Damen, K.C. Huang, J.P. Simorre, E. Breukink, T. den Blaauwen, A. Typas, C.A. Gross, W. Vollmer, Coordination of peptidoglycan synthesis and outer membrane constriction during *Escherichia coli* cell division, elife 4 (2015), e07118.
8. G. Guihard, P. Boulanger, H. Bénédetti, R. Lloubés, M. Besnard, L. Letellier, Colicin A and the Tol proteins involved in its translocation are preferentially located in the contact sites between the inner and outer membranes of *Escherichia coli* cells, J. Biol. Chem. 269 (1994) 5874-5880.
9. R. Derouiche, H. Bénédetti, J.C. Lazzaroni, C. Lazdunski, R. Lloubes, Protein complex within *Escherichia coli* inner membrane. TolA N-terminal domain interacts with TolQ and TolR proteins, J. Biol. Chem. 270 (1995) 11078-11084.
10. E. Bouveret, R. Derouiche, A. Rigal, R. Lloubes, C. Lazdunski, H. Bénédetti, Peptidoglycan-associated lipoprotein-TolB interaction, A possible key to explaining the formation of contact sites between the inner and outer membranes of *Escherichia coli,* J. Biol. Chem. 270 (1995) 11071-11077.

11. E. Bouveret, H. Bénédetti, A. Rigal, E. Loret, C. Lazdunski, *In vitro* characterization of peptidoglycan-associated lipoprotein (PAL)-peptidoglycan and PAL-TolB interactions, J. Bacteriol. 181 (1999) 6306-6311.
12. A. Walburger, C. Lazdunski, Y. Corda, The Tol/Pal system function requires an interaction between the C-terminal domain of TolA and the N-terminal domain of TolB, Mol. Microbiol. 44 (2002) 695-708.
13. M.A. Gerding, Y. Ogata, N.D. Pecora, H. Niki, P.A. de Boer, The trans-envelope Tol-Pal complex is part of the cell division machinery and required for proper outer-membrane invagination during cell constriction in *E. coli*, Mol. Microbiol. 63 (2007) 1008-1025.
14. E. Cascales, R. Lloubes, J.N. Sturgis, The TolQ-TolR proteins energize TolA and share homologies with the flagellar motor proteins MotA-MotB, Mol. Microbiol. 42 (2001) 795-807.
15. T Minamino, K Imada, The bacterial flagellar motor and its structural diversity, Trends Microbiol. 23 (2015) 267-274.
16. H. Celia, N. Noinaj, S.D. Zakharov, E. Bordignon, I. Botos, M. Santamaria, T.J. Barnard, W.A. Cramer, R. Lloubes, S.K. Buchanan, Structural insight into the role of the Ton complex in energy transduction, Nature 538 (2016) 60-65.
17. R. Agrebi, M. Wartel, C. Brochier-Armanet, T. Mignot, An evolutionary link between capsular biogenesis and surface motility in bacteria, Nat. Rev. Microbiol. 13 (2015) 318-326.
18. A.J. Heilpern, M.K. Waldor, CTXphi infection of *Vibrio cholerae* requires the *tolQRA* gene products, J Bacteriol. 182 (2000) 1739-1747.
19. J.F. Dubuisson, A. Vianney, N. Hugouvieux-Cotte-Pattat, J.C. Lazzaroni, Tol-Pal proteins are critical cell envelope components of *Erwinia chrysanthemi* affecting cell morphology and virulence, Microbiology. 151 (2005) 3337-3347.
20. G.K. Paterson, H. Northen, D.B. Cone, C. Willers, S.E. Peters, D.J. Maskell, Deletion of *tolA* in *Salmonella Typhimurium* generates an attenuated strain with vaccine potential, Microbiology. 155 (2009) 220-228.
21. Y.C. Yeh, L.R. Comolli, K.H. Downing, L. Shapiro, H.H. McAdams, The caulobacter Tol-Pal complex is essential for outer membrane integrity and the positioning of a polar localization factor, J. Bacteriol. 192 (2010) 4847-4858.

22. T.M. Santos, T.Y. Lin, M. Rajendran, S.M. Anderson, D.B. Weibel, Polar localization of *Escherichia coli* chemoreceptors requires an intact Tol-Pal complex, Mol. Microbiol. 92 (2014) 985-1004.
23. R. Shrivastava, X. Jiang, S.S. Chng, Outer membrane lipid homeostasis via retrograde phospholipid transport in *Escherichia coli*. Mol. Microbiol. 106 (2017) 395-408.
24. L. Houot, R. Navarro, M. Nouailler, D. Duché, F. Guerlesquin, R. Lloubes, Electrostatic interactions between the CTX phage minor coat protein and the bacterial host receptor TolA drive the pathogenic conversion of *Vibrio cholerae*, J. Biol. Chem. 292 (2017) 13584-13598.
25. J. Meury, G. Devilliers, Impairment of cell division in *tolA* mutants of *Escherichia coli* at low and high medium osmolarities, Biol. Cell. 91 (1999) 67-75.
26. E. Cascales, S.K. Buchanan, D. Duché, C. Kleanthous, R. Lloubes, K. Postle, M. Riley, S. Slatin, D. Cavard, Colicin biology, Microbiol. Mol. Biol. Rev. 71 (2007) 158-229.
27. T. Dinh, T.G. Bernhardt, Using superfolder green fluorescent protein for periplasmic protein localization studies, J Bacteriol. 193 (2011) 4984-4987.
28. D.A. Bonsor, O. Hecht, M. Vankemmelbeke, A. Sharma, A.M. Krachler, N.G. Housden, K.J. Lilly, R. James, G.R. Moore, C. Kleanthous, Allosteric beta-propeller signalling in TolB and its manipulation by translocating colicins, EMBO J. 28 (2009) 2846-57. Erratum in: EMBO J. 28: 2858.
29. J.C. Lazzaroni, R.C. Portalier, Genetic and biochemical characterization of periplasmic-leaky mutants of *Escherichia coli* K-12, J. Bacteriol. 145 (1981) 1351-1358.
30. J.K. Davies, P. Reeves, Genetics of resistance to colicins in *Escherichia coli* K-12: cross-resistance among colicins of group A, J. Bacteriol. 123 (1975) 102-107.
31. A. Vianney, M.M. Muller, T. Clavel, J.C. Lazzaroni, R. Portalier, R.E. Webster, Characterization of the *tol-pal* region of *Escherichia coli* K-12: translational control of tolR expression by TolQ and identification of a new open reading frame downstream of pal encoding a periplasmic protein, J Bacteriol. 178 (1996) 4031-4038.
32. P. Germon, T. Clavel, A. Vianney, R. Portalier, J.C. Lazzaroni, Mutational analysis of the *Escherichia coli* K-12 TolA N-terminal region and characterization

of its TolQ-interacting domain by genetic suppression, J. Bacteriol. 180 (1998) 6433-6439.

33. A. Bernadac, M. Gavioli, J-C. Lazzaroni, S. Raina, R. Lloubes, *Escherichia coli tol-pal* mutants form outer membrane vesicles, J. Bacteriol. 180 (1998) 4872-4878.

34. R. Lloubes, A. Bernadac, L. Houot, S. Pommier, Non classical secretion systems,
Res Microbiol. 164 (2013) 655-663.

35. E.L. Goemaere, E. Cascales, R. Lloubes, Mutational analyses define helix organization and key residues of a bacterial membrane energy-transducing complex. J. Mol. Biol. 366 (2007) 1424-1436.

36. T. Clavel, P. Germon, A. Vianney, R. Portalier, J.C. Lazzaroni, TolB protein of *Escherichia coli* K-12 interacts with the outer membrane peptidoglycan-associated proteins Pal, Lpp and OmpA, Mol. Microbiol. 29 (1998) 359-67.

37. M.A. Teleha, A.C. Miller, R.A. Larsen, Overexpression of the *Escherichia coli* TolQ protein leads to a null-FtsN-like division phenotype, Microbiologyopen. 2 (2013) 618-632.

38. C.S. Bernard, M. Sadasivam, D. Shiomi, W. Margolin, An altered FtsA can compensate for the loss of essential cell division protein FtsN in *Escherichia coli*, Mol. Microbiol. 64 (2007) 1289-1305.

39. E. Cascales, R. Lloubes, Deletion analyses of the peptidoglycan-associated lipoprotein Pal reveals three independent binding sequences including a TolA box, Mol. Microbiol. 51 (2004) 873-85.

40. A. Typas, M. Banzhaf, B. van den Berg van Saparoea, J. Verheul, J. Biboy, R.J. Nichols, M. Zietek, K. Beilharz, K. Kannenberg, M. von Rechenberg, E. Breukink, T. den Blaauwen, C.A. Gross, W. Vollmer, Regulation of peptidoglycan synthesis by outer-membrane proteins. Cell. 143 (2010) 1097-1109.

41. F. Van den Ent, J. Löwe, RF cloning: a restriction-free method for inserting target genes into plasmids, J. Biochem. Biophys. Methods. 67 (2006) 67-74.

42. K.A. Datsenko, B.L. Wanner, One-step inactivation of chromosomal genes in *Escherichia coli* K-12 using PCR products, Proc. Natl. Acad. Sci. U. S. A. 97 (2000) 6640-6645.

43. M-S. Aschtgen, C.S. Bernard, S. De Bentzmann, R. Lloubes, E. Cascales, SciN is an outer membrane lipoprotein required for type VI secretion in enteroaggregative *Escherichia coli,* J. Bacteriol. 190 (2008) 7523-7531.
44. L. Journet, E. Bouveret, A. Rigal, R. Lloubes, C. Lazdunski, H., Bénédetti, Import of colicins across the outer membrane of *Escherichia coli* involves multiple protein interactions in the periplasm, Mol. Microbiol. 42 (2001) 331-344.
45. C.L. Santini, A. Bernadac, M. Zhang, A. Chanal, B. Ize, C. Blanco, L.F. Wu, Translocation of jellyfish green fluorescent protein via the Tat system of *Escherichia coli* and change of its periplasmic localization in response to osmotic up-shock, J. Biol. Chem. 276 (2001) 8159-8164.
46. B.J. Bachmann, Pedigrees of some mutant strains of *Escherichia coli* K-12, Bacteriol Rev. 36 (1972) 525-557.
47. E. Durand, V.S. Nguyen, A. Zoued, L. Logger, G. Péhau-Arnaudet, M.S. Aschtgen, S. Spinelli, A. Desmyter, B. Bardiaux, A. Dujeancourt, A. Roussel, C. Cambillau, E. Cascales, R. Fronzes, Biogenesis and structure of a type VI secretion membrane core complex, Nature 523 (2015) 555-560.
48. Y.R. Brunet, A. Khodr, L. Logger, L. Aussel, T. Mignot, S. Rimsky, E. Cascales, H-NS Silencing of the Salmonella Pathogenicity Island 6-Encoded Type VI Secretion System Limits *Salmonella enterica* Serovar Typhimurium Interbacterial Killing, Infect. Immun. 83 (2015) 2738-2750.
49. M.K. Chaveroche, J.M. Ghigo, C. d'Enfert. A rapid method for efficient gene replacement in the filamentous fungus *Aspergillus nidulans*, Nucleic Acids Res. 28 (2000) E97.

Figures legends

Fig. 1. The *Escherichia coli tol-pal* gene cluster. (a) Schematic representation of the components of the Tol-Pal complex in the *Escherichia coli* envelope. (b) Organization of the *tol-pal* operons. The genes are represented by arrowheads. The two promoters and the inserts encoding sfGFP or mCherry fusions are indicated by arrows.

Fig. 2. Chromosomal encoded Tol-Pal fusion proteins are functional. (a) Sensitivity to SDS of WT, sfGFP-TolA and ΔTolA cells (strains are referenced in Table S1) was tested in liquid LB medium containing various concentrations of SDS at 37°C. The percentage of surviving cells in liquid LB medium was estimated after 4 hours from the turbidity ratio of the SDS-treated and the control sample. Error bars indicate the error on triplicate samples for each condition. (b) Phase contrast imaging of WT, sfGFP-TolA and ΔTolA strains showing cell division defect or not after growth at 37°C in LB (upper panel) or in LB without NaCl (lower panel). Any of the *tol-pal* gene deletion leads to cell septation defect under hypo-osmolarity conditions. Scale Bar: 5 µm. (c) Sensitivity of WT, GFP-TolA and ΔTolA strains to colicin A (Tol dependent) and colicin D (Ton dependent) lethal activities was tested using dilutions from 10^{-1} to 10^{-4} of colicins spotted on freshly seeded lawns. Zones of clearance indicate colicins activity against the strain. (d) Western blot analysis was used to check native and chimeric Tol-Pal protein production in each *tol-pal* chromosomal fusion strain. The antibodies used are indicated.

Fig. 3. The Tol-Pal proteins localize to cell septum during cell division. (a) Fluorescent microscopy time-lapse recording of *E. coli* W3110 cells expressing the fluorescent versions the Tol-Pal proteins. Individual images were taken every 4 min. Corresponding kymograph of each time-lapse is shown on left panel. Dark areas are outside the cell. Note that protein fluorescence re-localizes to future division sites. (b) Fluorescent profiles (demographs) of *E. coli* W3110 cells expressing the fluorescent versions the Tol-Pal proteins where n represents the number of cells for a triplicate study. The signal intensity in each cell is represented by a color code, from dark blue

(low intensity) to yellow (high intensity). On the y-axis, cells are sorted for length, ascending from top (the shortest cell) to down (the longest cell). Each horizontal line corresponds to a single cell. The longest cells correspond to cells in the last stage of cell division. In all these experiments, *E. coli* W3110 wild-type or derivative strains, were grown in M9 minimal medium supplemented with glucose and casa-amino acids at 30°C.

Fig. 4. Localization of the membrane Tol-Pal proteins in different genetic backgrounds. Fluorescence microscopy images of the different IM fluorescent Tol proteins were observed in each *tol-pal* gene deletion background. (a) TolQ-mCherry, (b) sfGFP-TolR, (c) sfGFP-TolA. Note that the three proteins are able to localize at constriction sites during cell division independently of their Tol-Pal partners. Heatmap distribution in cells of the fluorescent proteins tested is represented on the right of each panel where n represents the number of cells for each study. Scale Bar: 2 µm. In all these experiments, *E. coli* W3110 wild-type or derivative strains, were grown in M9 minimal medium supplemented with glucose and casa-amino acids at 30°C.

Fig. 5. Localization of the outer-membrane Tol-Pal complex in different genetic backgrounds**.** (a) Fluorescence microscopy images of W3110 *E. coli* cells expressing the chromosomal fluorescent fusion protein TolB-mCherry or the plasmid encoded Tat-GFP fusion protein. Tat-GFP has been previously described to be efficiently exported across the IM by the Twin-arginine transport system [45]. Tat-GFP is observed in the periplasm of the producing cells whereas TolB-mCherry localizes at constriction sites during cell division. Heatmap distribution in cells of the fluorescent proteins tested is represented on the right of each panel where n represents the number of cells for each study. Scale Bar: 2 µm. (b) Fluorescence microscopy images of *tol-pal* mutants cells producing Tat-GFP and TolB-mCherry. In *tol-pal* mutants, fluorescence is observed in vesicles at cell poles or cell septa. Accumulation of Tat-GFP or TolB-mCherry in vesicles is indicated by arrows. (c) Fluorescence microscopy images of W3110 cells expressing the chromosomal fusion protein Pal-mCherry in different genetic backgrounds. As shown previously, Pal-mCherry is observed at midcell in a wild type background. Localization at cell septum is affected in a Δ*tolA*, Δ*tolQR and* Δ*tolB* mutant. In a Δ*tolQR* mutant carrying the

plasmid pTolQR encoding TolQ and TolR, Pal-mCherry localization at the cell septum is restored. In a ΔtolQR mutant carrying the plasmid pTolQR$_{D23A}$ encoding TolQ and TolR$_{D23A}$, Pal-mCherry does not localize at the cell septum but appears dispersed in the cell envelope. In all these experiments, *E. coli* W3110 wild-type or derivative strains, were grown in M9 minimal medium supplemented with glucose and casa-amino acids at 30°C.

Fig. 6. Localization and function of Pal variants. (a) Western blot analysis of Pal, Pal-sfGFP, Pal$_{102}$-sFGP and Pal$_{104}$-sfGFP production. Bacteria constitutively producing or not Pal and producing plasmid encoding Pal-sfGFP, Pal$_{102}$-sFGP and Pal$_{104}$-sfGFP were grown in LB medium at 37°C to an A_{600} = 0.3 and induced for 60 min with 0.02% arabinose. Cell extracts (A_{600} = 0.2) were immunoblotted and the presence or absence of the protein of interest was detected with anti-Pal antibodies. (b) Phase contrast imaging of strains producing Pal-sfGFP, Pal$_{102}$-sFGP and Pal$_{104}$-sfGFP showing cell division after growth at 37°C in LB (upper panel) or in LB - NaCl (lower panel). Scale Bar: 5 µm. (c) Sensitivity to SDS of W3110, Δ*pal*, and Δ*pal* strains producing Pal-sfGFP, Pal$_{102}$-sFGP and Pal$_{104}$-sfGFP was tested in liquid LB medium containing various concentrations of SDS. The percentage of surviving cells in liquid LB medium was estimated after 4 hours of growth at 37°C from the turbidity ratio of the SDS-treated and the control sample. Error bars indicate the error on triplicate samples for each condition. (d) Schematic of Pal$_{E102K}$ and Pal$_{R104C}$ interactions with TolB and the PG previously published [36]. Pal$_{E102K}$ interacts with the PG but not with TolB, whereas Pal$_{R104C}$ interacts with TolB but not with the PG. (e) A Δ*pal* strain was complemented with pPal-sfGFP, pPal$_{E102K}$-sfGFP or pPal$_{R104C}$-sfGFP. *E. coli* W3110 wild-type or derivative strains were grown in M9 minimal medium supplemented with glucose and casa-amino acids at 30°C. Fluorescence microscopy images reveal that Pal-sfGFP and Pal$_{R104C}$-sfGFP localize at the cell septum during cell division in contrast to Pal$_{E102K}$-sfGFP. The septal localization of Pal$_{R104C}$-sfGFP is abolished in a Δ*tolB-pal* strain.

Table 1. Phenotypic analysis of *tol-pal* chromosomal fusions and deletions strains.
W3110 cells expressing different chromosomal fusions and deletions of the *tol-pal* genes were tested for level of import of colicin A (Tol dependent) and colicin D (Ton

dependent), susceptibility to SDS and cell division +/- NaCl. SDS sensitivity was tested in liquid LB medium containing various concentrations of SDS (R: resistant, S: sensitive). Colicin A and D sensitivity was tested on bacterial lawns by a spot dilution assay. The number indicated represents the maximal 10-fold dilution of the colicin stock (1 mg/ml) still able to kill the strain tested (0: resistant, 4: sensitive to 10^4 dilution). Cell division was observed during exponential phase after growth in LB or LB - NaCl (N = Normal cell division, C = Chain formation).

Table 1: *E. coli* strains and phenotypes.

Strains	OM stability SDS	Cell chaining	Colicin uptake A	D
W3110	R	N	4	4
sfGFP-TolA	R	N	4	4
sfGFP-TolR	R	N	4	4
TolQ-mCherry	R	N	4	4
TolB-mCherry	R	N	4	4
Pal-mCherry	R	N	4	4
ΔTolA	S	C	0	4
ΔTolQ	S	C	0	4
ΔTolR	S	C	0	4
ΔTolQR	S	C	0	4
ΔTolB	S	C	0	4
ΔPal	S	C	4	4
ΔTolB-Pal	S	C	0	4
sfGFP-TolA:ΔTolQR	S	C	0	4
sfGFP-TolA:ΔTolB	S	C	0	4
sfGFP-TolA:ΔPal	S	C	4	4
sfGFP-TolR:ΔTolA	S	C	0	4
sfGFP-TolR:ΔTolQ	S	C	0	4
sfGFP-TolR:ΔTolB	S	C	0	4
sfGFP-TolR:ΔPal	S	C	4	4
TolQ-mCherry:ΔTolA	S	C	0	4
TolQ-mCherry:ΔTolR	S	C	0	4
TolQ-mCherry:ΔTolB	S	C	0	4
TolQ-mCherry:ΔPal	S	C	4	4
TolB-mCherry:ΔTolA	S	C	0	4
TolB-mCherry:ΔTolQR	S	C	0	4
TolB-mCherry:ΔPal	S	C	4	4
Pal-mCherry: ΔTolA	S	C	0	4
Pal-mCherry: ΔTolQR	S	C	0	4
Pal-mCherry: ΔTolB	S	C	0	4
Pal-mCherry: ΔTolQR pTolQR	R	N	4	4
Pal-mCherry: ΔTolQR pTolQR$_{D23A}$	S	C	0	4
ΔPal: pPal-sfGFP	R	N	4	4
ΔPal: pPal$_{E102K}$-sfGFP	S	C	4	4
ΔPal: pPal$_{R104C}$-sfGFP	S	C	4	4

Supplemental information

Fig. S1. Sensitivity to SDS of WT and derivative mutant strains. Sensitivity to SDS of the indicated strains was tested in liquid LB medium containing various concentrations of SDS: 0.25% to 2%. The percentage of surviving cells in liquid LB medium was estimated after 4 hours at 37°C from the turbidity ratio of the SDS-treated and the control sample. Error bars indicate the error on triplicate samples for each condition.

Fig. S2. Phase contrast imaging of WT and derivative mutant strains. Phase contrast imaging of WT and modified strains showing cell division after growth at 37°C in LB (right panel) or in LB - NaCl (left panel). *tol-pal* gene deletions lead to cell septation defect in hypo-osmolarity conditions. In contrast all the strains encoding the fluorescent Tol-Pal fusion proteins present a wild-type phenotype. Scale Bar: 2.5 µm

Fig. S3. Sensitivity to colicins of WT and derivative mutant strains. Sensitivity of WT and modified strains to colicin A (Tol dependent) and colicin D (Ton dependent) lethal activities was tested using dilutions from 10^{-1} to 10^{-4} of colicins spotted on freshly seeded lawns. Zones of clearance indicate colicins activity against the strain. Colicin D uses the TonB system to enter and to kill cells and its lethal activity is not affected by a *tol-pal* deletion. Pal is not required for colicin A mode of action in contrast to the other Tol proteins. Note that all the strains encoding the fluorescent Tol-Pal fusion proteins are sensitive to the colicin A.

Fig. S4. Tol-Pal proteins production in the different modified strains. Western blot analysis was used to check native and chimeric Tol-Pal proteins production in each *tol-pal* chromosomal fusion and deletion strain. The antibodies used are indicated on the left.

Table S1: *E. coli* strains and plasmids.

Strains or plasmids	Genotype	Source
Strains		
W3110	F'λ^{-}*IN(rrnD-rrnE)1 rph-1*	[46]
sfGFP-TolA	W3110 *sfGFP-tolA::frt*	This study
sfGFP-TolR	W3110 *sfGFP-tolR::frt*	This study
TolQ-mCherry	W3110 *tolQ-mCherry::frt*	This study
TolB-mCherry	W3110 *tolB-mCherry::frt*	This study
Pal-mCherry	W3110 *pal-mCherry::frt*	This study
ΔTolA	W3110 Δ*tolA::frt*	This study
ΔTolQ	W3110 Δ*tolQ::frt*	This study
ΔTolR	W3110 Δ*tolR::frt*	This study
ΔTolQR	W3110 Δ*tolQR::frt*	This study
ΔTolB	W3110 Δ*tolB::frt*	This study
ΔPal	W3110 Δ*pal::frt*	This study
ΔTolB-Pal	W3110 Δ*tolB-pal::frt*	This study
sfGFP-TolA:ΔTolQR	W3110 *sfGFP-tolA::frt*, Δ*tolQR::kan*	This study
sfGFP-TolA:ΔTolB	W3110 *sfGFP-tolA::frt*, Δ*tolB::kan*	This study
sfGFP-TolA:ΔPal	W3110 *sfGFP-tolA::frt*, Δ*pal::kan*	This study
sfGFP-TolR:ΔTolA	W3110 *sfGFP-tolR::frt*, Δ*tolA::kan*	This study
sfGFP-TolR:ΔTolQ	W3110 *sfGFP-tolR::frt*, Δ*tolQ::kan*	This study
sfGFP-TolR:ΔTolB	W3110 *sfGFP-tolR::frt*, Δ*tolB::kan*	This study
sfGFP-TolR:ΔPal	W3110 *sfGFP-tolR::frt*, Δ*pal::kan*	This study
TolQ-mCherry:ΔTolA	W3110 *tolQ-mCherry:: frt*, Δ*tolA::kan*	This study
TolQ-mCherry:ΔTolR	W3110 *tolQ-mCherry::frt*, Δ*tolR::kan*	This study
TolQ-mCherry:ΔTolB	W3110 *tolQ-mCherry::frt,* Δ*tolB::kan*	This study
TolQ-mCherry:ΔPal	W3110 *tolQ-mCherry::frt*, Δ*pal::kan*	This study
TolB-mCherry:ΔTolA	W3110 *tolB-mCherry::frt*, Δ*tolA::kan*	This study
TolB-mCherry:ΔTolQR	W3110 *tolB-mCherry::frt*, Δ*tolQR::kan*	This study
TolB-mCherry:ΔPal	W3110 *tolB-mCherry::frt*, Δ*pal::kan*	This study
Pal-mCherry: ΔTolA	W3110 *pal-mCherry::frt,* Δ*tolA::kan*	This study
Pal-mCherry: ΔTolQR	W3110 *pal-mCherry::frt,* Δ*tolQR::kan*	This study
Pal-mCherry: ΔTolB	W3110 *pal-mCherry::frt,* Δ*tolB::kan*	This study
Plasmids		
pBad/HisC	*amp*	Invitrogene
pKD4-mCherry	*kan*	[47]
psfGFP-KD4	*kan*	[48]
pCP20	*amp flp* recombinase	[42]
pKOBEG	*cm, λred* integrase	[49]
pTolQR	*amp*, pBad/HisC *tolQR*	This study
pTolQR$_{D23A}$	*amp*, pBad/HisC *tolQR$_{D23A}$*	This study
pPal-sfGFP	*amp*, pBad/HisC *pal-sfgfp*	This study
pPal$_{E102K}$-sfGFP	*amp*, pBad/HisC *pal$_{E102K}$-sfgfp*	This study
pPal$_{R104C}$-sfGFP	*amp*, pBad/HisC *pal$_{R104C}$-sfgfp*	This study
pTat-sfGFP	*amp*, pBAD24 *tat-gfp*	[45]

Figure
Click here to download high resolution image

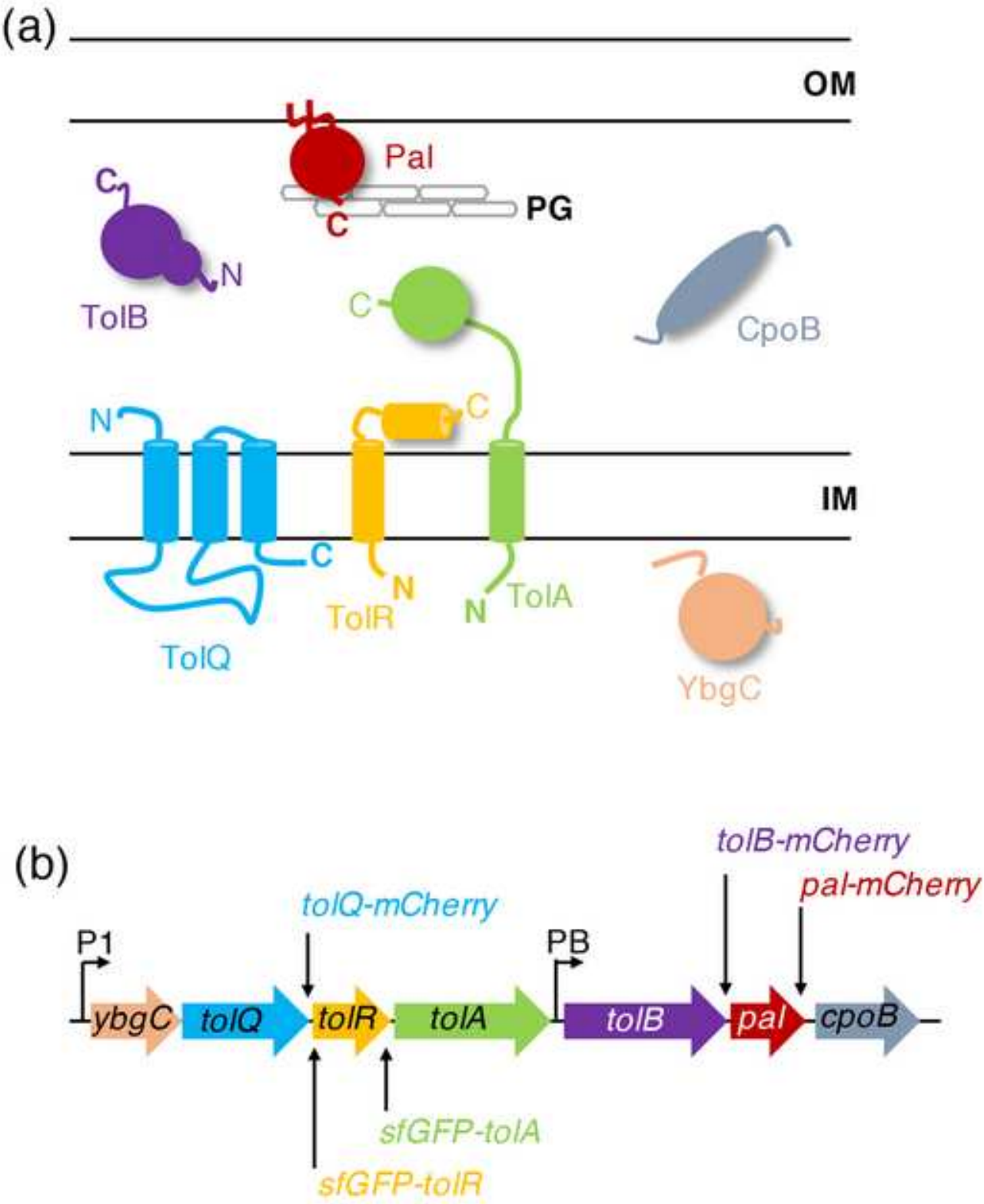

Figure
Click here to download high resolution image

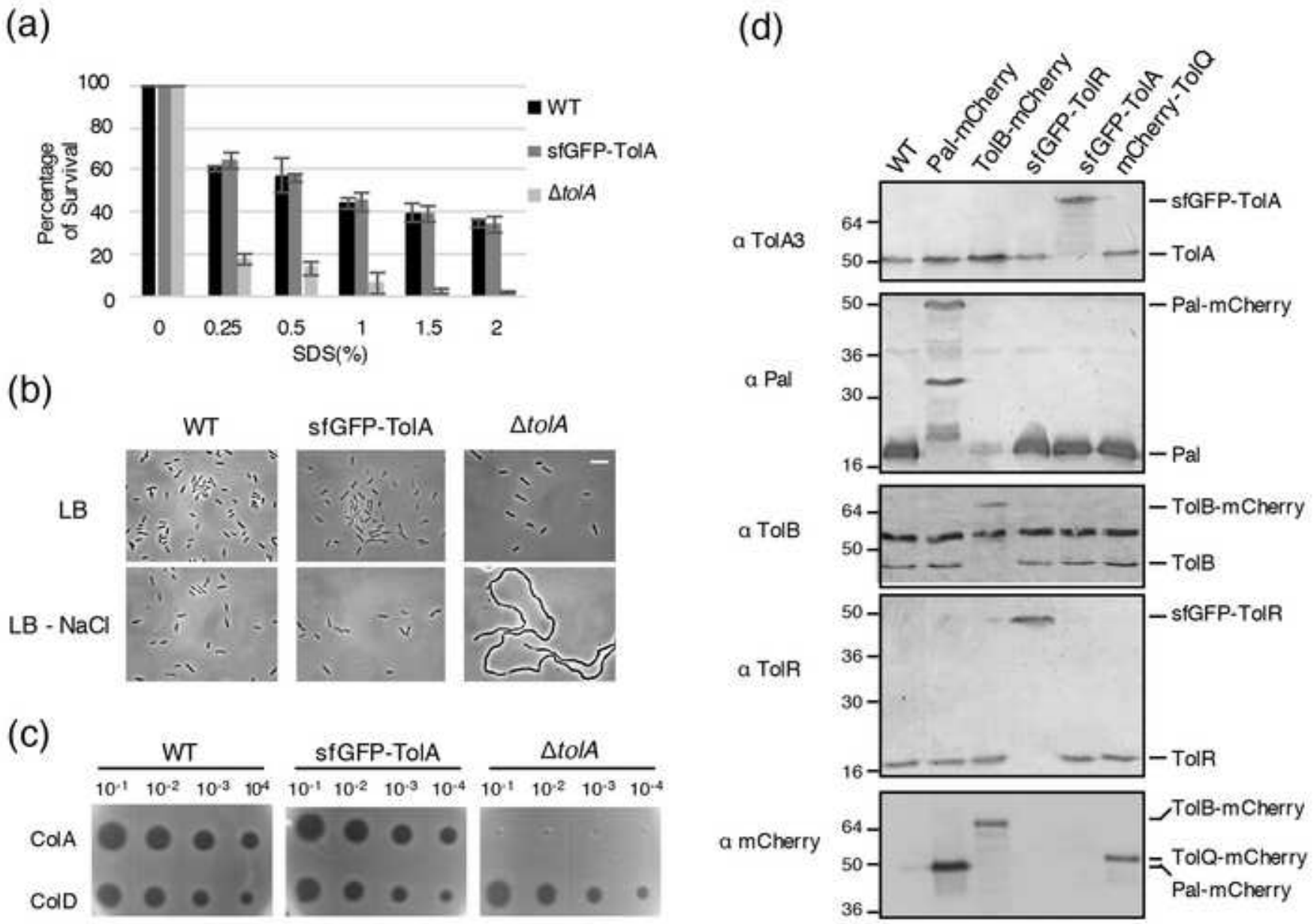

Figure
Click here to download high resolution image

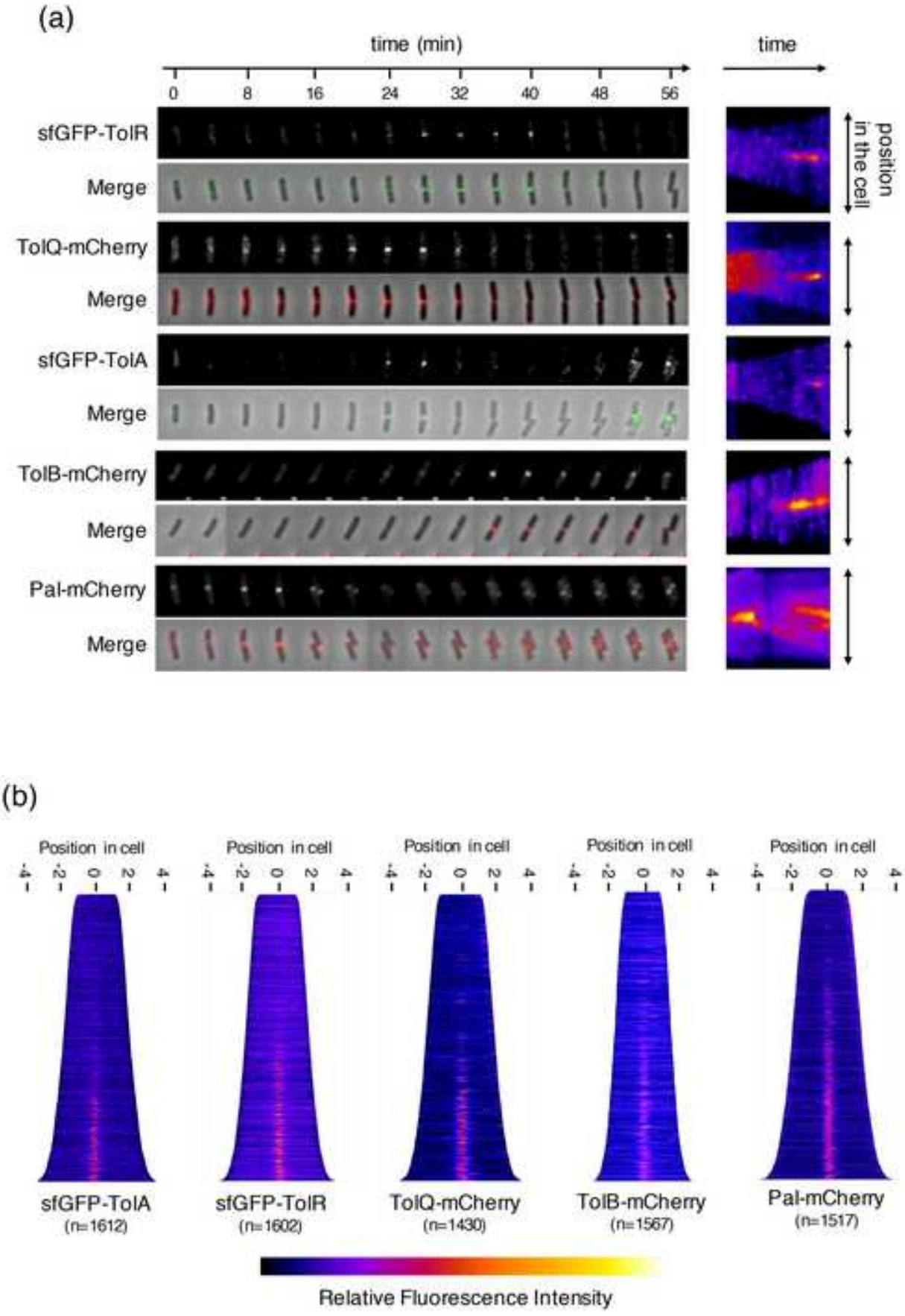

Figure
Click here to download high resolution image

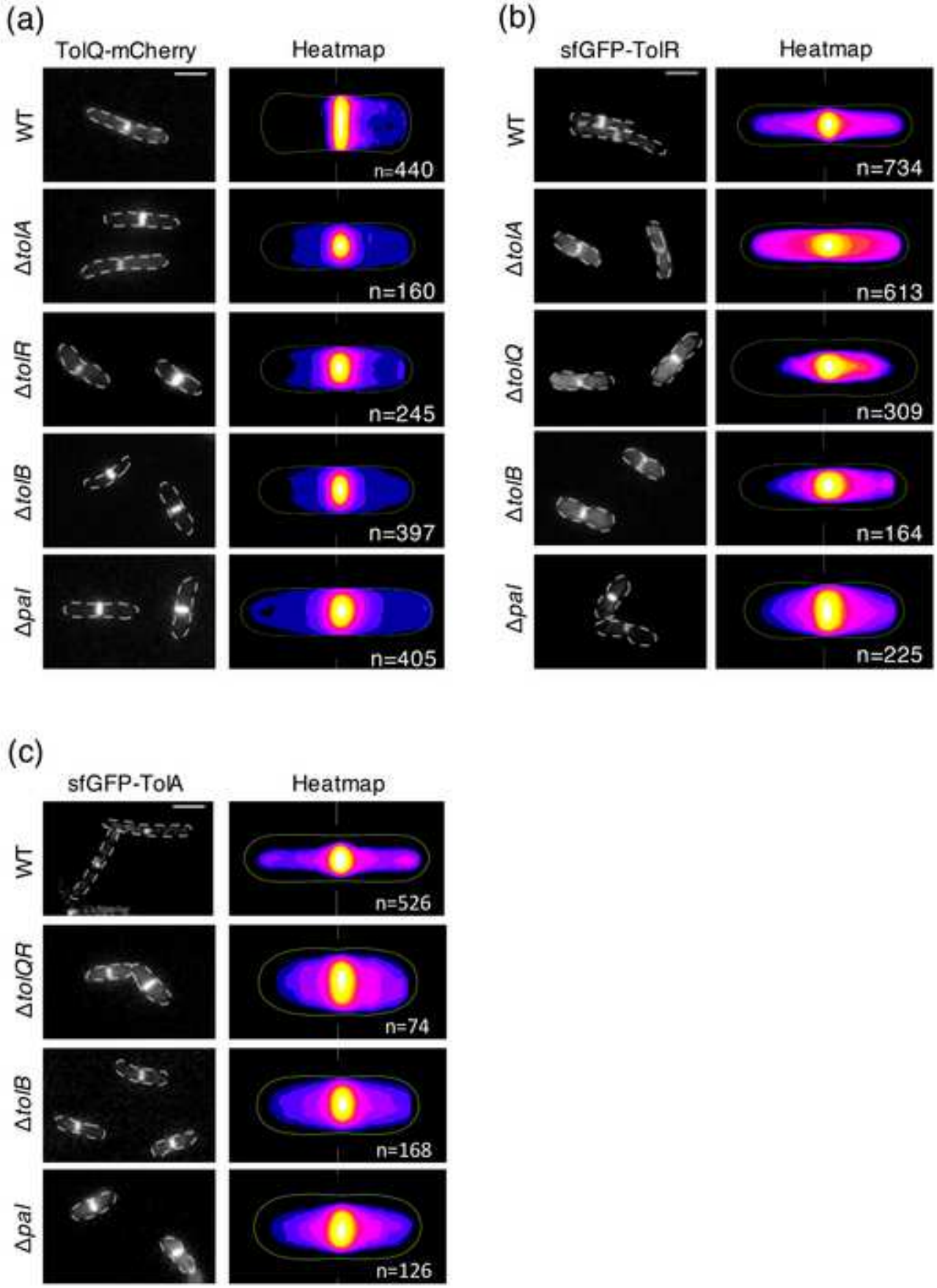

Figure
Click here to download high resolution image

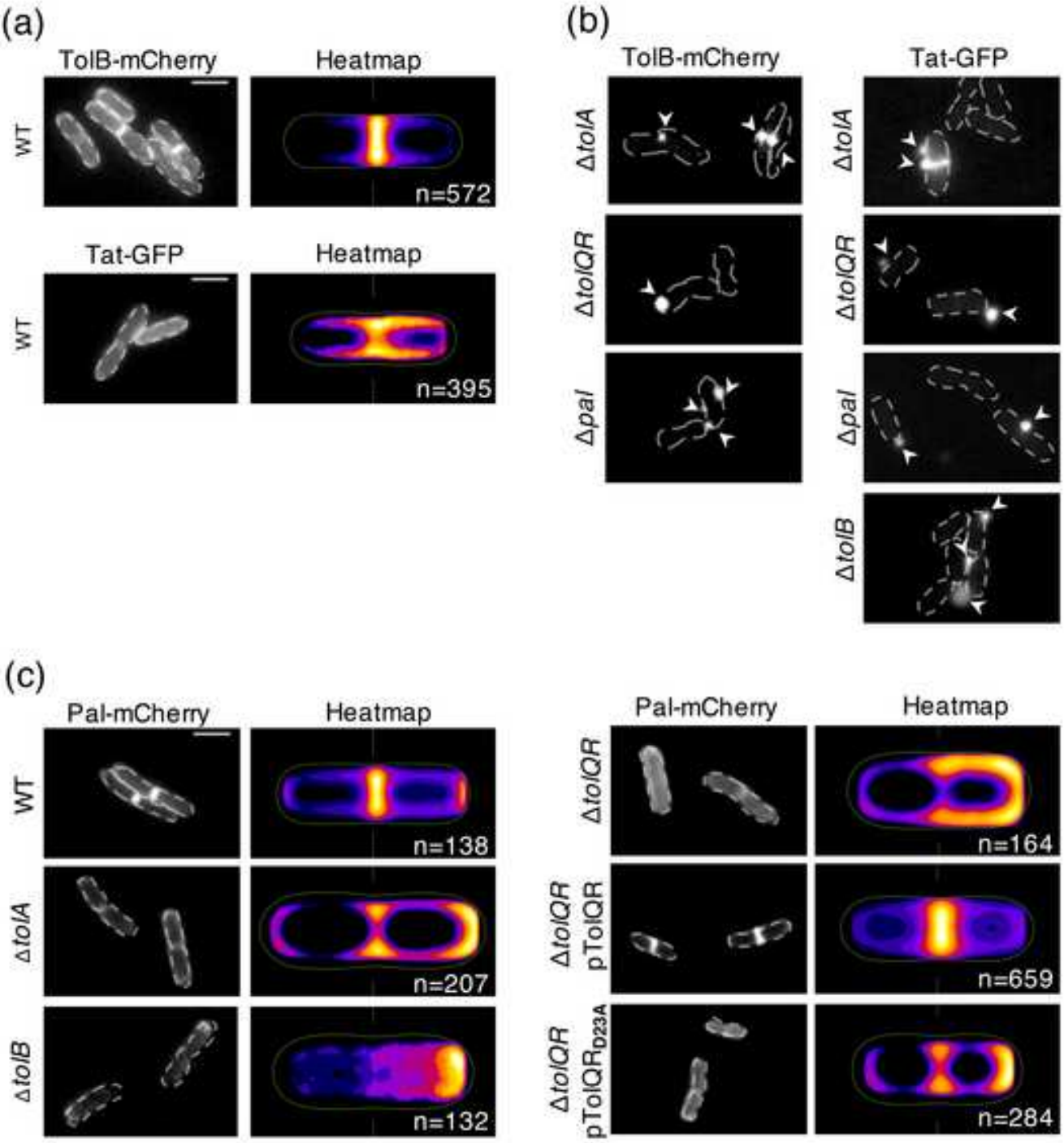

Figure
Click here to download high resolution image